

Dynamic instability analysis of laminated composite stiffened shell panels subjected to in-plane harmonic edge loading

S. N. Patel[†] and P. K. Datta[‡]

Department of Aerospace Engineering, I.I.T. Kharagpur, Kharagpur-721 032, India

A. H. Sheikh^{††}

Department of Ocean Engineering and Naval Architecture, I.I.T. Kharagpur, Kharagpur-721 032, India

(Received March 7, 2005, Accepted November 22, 2005)

Abstract. The dynamic instability characteristics of laminated composite stiffened shell panels subjected to in-plane harmonic edge loading are investigated in this paper. The eight-noded isoparametric degenerated shell element and a compatible three-noded curved beam element are used to model the shell panels and the stiffeners respectively. As the usual formulation of degenerated beam element is found to overestimate the torsional rigidity, an attempt has been made to reformulate it in an efficient manner. Moreover the new formulation for the beam element requires five degrees of freedom per node as that of shell element. The method of Hill's infinite determinant is applied to analyze the dynamic instability regions. Numerical results are presented to demonstrate the effects of various parameters like shell geometry, lamination scheme, stiffening scheme, static and dynamic load factors and boundary conditions, on the dynamic instability behaviour of laminated composite stiffened panels subjected to in-plane harmonic loads along the boundaries. The results of free vibration and buckling of the laminated composite stiffened curved panels are also presented.

Keywords: buckling; composite stiffened shell panels; degenerated curved beam element; degenerated shell element; dynamic instability; finite element method; in-plane load and vibration.

1. Introduction

A shell structure experiences in-plane forces in many situations. The presence of such loads significantly affects the free vibration characteristics of the structures. The buckling phenomenon may be considered as a particular case of free vibration problem with in-plane load, whereas the load approaches towards its critical value of buckling, the frequency of vibration tends to zero. When the in-plane load becomes harmonic, it may lead to the condition of parametric resonance. It is found that certain combinations of the frequency of pulsating in-plane force and the natural

[†] Research Scholar, E-mail: shuvendu_patel@yahoo.co.in

[‡] Professor, Corresponding author, E-mail: pkdatta@aero.iitkgp.ernet.in

^{††} Professor, E-mail: hamid@naval.iitkgp.ernet.in

frequencies of transverse vibration produce dynamic instability where the amplitude of the transverse vibration increases without bound. This phenomenon is entirely different from the usual resonance of forced vibration. In forced vibration when the frequency of the transverse forcing system matches with the natural frequency of the structure, resonance occurs. Thus the resonance phenomenon in forced vibration problem is relatively simple since the structure loses stability at constant frequencies of the transverse loads. On the other hand the instability in case of parametric resonance occurs over a range of frequencies of the in-plane force rather than a single value. Again parametric resonance of a structure may occur at load level much less than the static buckling load while the static instability of the structure sets in at the static buckling load values. Thus a structural component designed to withstand static buckling load may easily fail in an environment having periodic in-plane loading. So a designer ought to consider the parametric resonance aspect while dealing a structure subjected to dynamic loading atmosphere.

A good deal of work on dynamic instability of structures has been undertaken by many researchers in the past. Bolotin (1964) has presented the general theory of dynamic stability of various elastic systems and discussed the peculiarities of the phenomena of instability. The parametric instabilities of laminated composite plate subjected to uniform loading are studied by many researchers (Srinivasan and Chellapandi 1986, Chen and Yang 1990, Kwon 1991, Moorthy *et al.* 1990). The dynamic stability analysis of stiffened plates and shells are few in the literature. Thomas and Abbas (1983) have presented the vibration characteristics and dynamic stability of stiffened plates. The parametric resonance of stiffened rectangular plates is investigated by Duffield and Willems (1972). Merrit and Willems (1973) investigated the dynamic instability for skew stiffened plates. The dynamic stability of radially stiffened annular plates with radial stiffener subjected to in-plane force is investigated by Mermertas and Belek (1991). Liao and Cheng (1994) have given some results for dynamic instability of stiffened composite plates and shells with uniform in-plane forces. They have studied only one example of stiffened shell panel having cylindrical geometry. Recently Shrivastava *et al.* (2002) have investigated the dynamic instability of isotropic stiffened plates with uniform edge loadings. Studies on free vibration of isotropic stiffened plates and shells are available in the literature (Aksu 1982, Mukherjee and Mukhopadhyay 1987, Mukhopadhyay 1989, Nayak and Bandyopadhyay 2002, Olson and Hazell 1977, Samanta and Mukhopadhyay 2004, Zeng and Bert 2001). However, this is relatively less in case of laminated composite stiffened curved panels. It is worth mentioning that the authors failed to get any result on buckling of composite stiffened curved panels in the literature. Similarly, no results on dynamic instability analysis of doubly curved stiffened panels are available.

The use of composite material is steadily increasing in many activities of aerospace, mechanical, civil and marine engineering structures due to its high strength/stiffness-to-weight ratio. In addition to that, the specific strength/stiffness of a panel can be enhanced by the use of a suitable stiffened structural form. These benefits have been exploited in the study of stiffened composite shell panel structure considered in the present investigation. In order to model a shell panel without any significant approximation related to the representation of arbitrary shell geometry, structural deformation and other associated aspects, the isoparametric 3D degenerated shell element (Ahmad 1970, Zienkiewicz 1977) having eight nodes is used. Though the concept of 3D degenerated shell element was initially proposed for isotropic shell (Ahmad 1970) but it has been subsequently extended to the fiber reinforced laminated panels (Panda and Natarajan 1979). The present formulation differs from Panda and Natarajan (1979) in the treatment of mapping in the thickness direction. Panda and Natarajan (1979) have mapped the individual layers whereas the entire



Fig. 1(a) Parallel stacking schemes

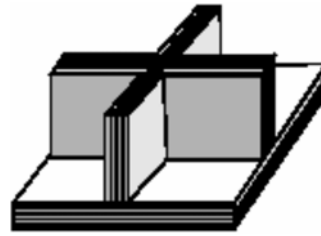


Fig. 1(b) Perpendicular stacking schemes

laminates is mapped in the present formulation. For the stiffeners, a compatible three-noded isoparametric curved beam element is used. The beam element is always placed along the edge of shell elements and this is intentionally not placed within the shell element in order to avoid the problem of stress jump within the shell element.

The basic concept underlying in the formulation of degenerated shell element (Ahmad 1970) has been extended to derive beam/stiffener elements having any arbitrary curve geometry suitable for use in two or three-dimensional problems (Ferguson and Clark 1979, Bathe 1996). Again the formulation for isotropic beam (Ferguson and Clark 1979, Bathe 1996) has been upgraded for laminated beam by Liao and Reddy (1990) where the stiffener layers are stacked parallel to those of the shell (parallel stacking scheme). Unfortunately the 3D degenerated beam element based on the above formulation (Bathe 1996, Ferguson and Clark 1979, Liao and Reddy 1990) has some problem in torsional mode since it overestimates torsional rigidity (Ferguson and Clark 1979). The problem becomes more severe in case of stiffeners having narrow cross-section like blade stiffener, which is quite common in composite construction. Keeping this aspect in view, the stiffener element is reformulated where the above mentioned problem has been eliminated by using torsion correction factor. In order to achieve that the stiffener bending in the plane of the shell surface is neglected. This should not affect the solution accuracy since deformation of the stiffener in that plane will be very small due to high in-plane rigidity of the shell skin. Moreover, the new formulation has the advantage that it requires five degrees of freedom per node while it is six in case of existing formulation (Bathe 1996, Ferguson and Clark 1979, Liao and Reddy 1990). Actually the stiffener element will directly share the five nodal unknowns of the shell element. The beam element considered has a rectangular section where provision has been kept for parallel (Fig. 1a) as well as perpendicular stacking schemes (Fig. 1b).

In the present study free vibration, buckling and dynamic instability analyses are carried out for different types of stiffened shell panels such as flat plate, cylindrical shell panel, spherical shell panel and hyperbolic paraboloid shell panel. The dynamic instability behaviours with respect to various parameters like shell geometry, lamination scheme, stiffening scheme, static and dynamic load factors for simply supported boundary conditions of laminated composite stiffened shell panels with in-plane harmonic edge loads are investigated in this study.

2. Theory and formulation

It has been mentioned in the previous section that the laminated stiffened panel structure is modeled by finite element technique. In order to have a better representation, the shell skin and

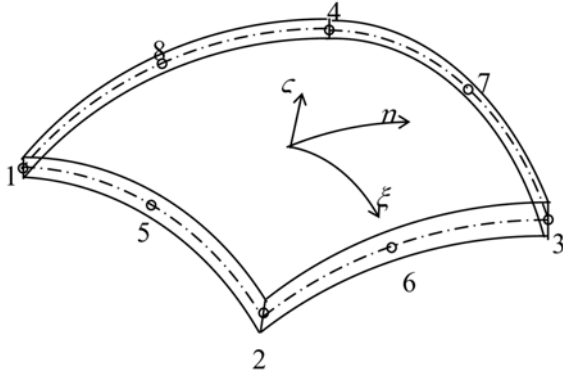


Fig. 2(a) Eight-noded quadrilateral degenerated shell element in curvilinear coordinates

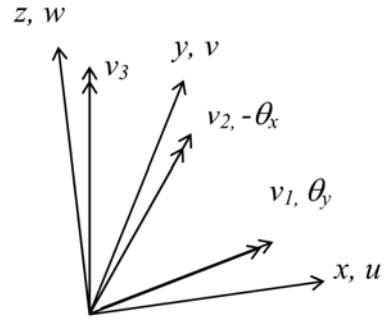


Fig. 2(b) Global cartesian coordinate (x, y and z) and nodal vector system at any node i

stiffeners are modeled as discrete/separate elements. The formulation of these elements is presented below.

2.1 Shell element

The formulation of the shell element is based on the basic concept of Ahmed *et al.* (1970), where the three-dimensional solid element used to model the shell is degenerated with the help of certain extractions obtained from the consideration that one of the dimension across the shell thickness is sufficiently small compared to other dimensions (Fig. 2). The detail derivation of this element for isotropic case is available in the literature (Ahmad 1970, Zienkiewicz 1977, Rao 1999).

The element geometry can be nicely represented by the natural coordinate system (ξ - η - ζ) where the curvilinear coordinates (ξ - η) are in the shell mid-surface while ζ is linear coordinate in the thickness direction. According to the isoparametric formulation, these coordinates (ξ , η and ζ) will vary from -1 to $+1$. With these, the coordinates of any point within the element may be expressed as

$$\begin{Bmatrix} x \\ y \\ z \end{Bmatrix} = \sum N_i \begin{Bmatrix} x_i \\ y_i \\ z_i \end{Bmatrix} + \sum N_i \frac{\zeta h_i}{2} \begin{Bmatrix} l_{3i} \\ m_{3i} \\ n_{3i} \end{Bmatrix} = \sum N_i \{X_i\} + \sum N_i \frac{\zeta h_i}{2} \{v_{3i}\} \tag{1}$$

where N_i are the quadratic serendipity shape functions in (ξ , η) plane, h_i is the thickness at the nodal points, $\{X_i\}$ are cartesian coordinates at mid-surface nodal points and $\{v_{3i}\}$ is the nodal vectors along the thickness direction.

The displacement field may be defined in terms of three displacements components (u_i , v_i and w_i) and two rotational components (θ_{xi} and θ_{yi}) at the mid-surface nodes (Fig. 2) as follows

$$\begin{Bmatrix} u \\ v \\ w \end{Bmatrix} = \sum_{i=1}^8 N_i \begin{Bmatrix} u_i \\ v_i \\ w_i \end{Bmatrix} - \sum_{i=1}^8 N_i \frac{\zeta h_i}{2} \begin{bmatrix} l_{1i} & l_{2i} \\ m_{1i} & m_{2i} \\ n_{1i} & n_{2i} \end{bmatrix} \begin{Bmatrix} \theta_{xi} \\ \theta_{yi} \end{Bmatrix} = [N_D] \{ \delta \} \tag{2}$$

where the displacements components (u_i , v_i and w_i) are taken along cartesian coordinate system (x, y

and z) and the rotational components (θ_{xi} and θ_{yi}) are taken about two mutually perpendicular lines tangential to the mid-surface (not necessarily follow ξ - η) having unit vectors as follows

$$\begin{aligned} \{v_{1i}\} &= [l_{1i} \ m_{1i} \ n_{1i}]^T \\ \{v_{2i}\} &= [l_{2i} \ m_{2i} \ n_{2i}]^T \end{aligned} \tag{3}$$

In the above Eq. (2), $\{\delta\}$ is the nodal displacement vector of an element and it is

$$\{\delta\} = [u_1 \ v_1 \ w_1 \ \theta_{x1} \ \theta_{y1} \ u_2 \ v_2 \ \dots \ \dots \ \theta_{y8}]^T \tag{4}$$

With the help of Eqs. (1) and (2) and following the steps of Ahmed *et al.* (1970), the strain-displacement relation along $(x'$ - y' - $z')$ can be expressed in terms of $\{\delta\}$ as

$$\{\varepsilon'\} = [B]\{\delta\} \tag{5}$$

where x' , y' and z' are taken along the directions of the above mentioned unit vectors v_1 , v_2 and v_3 respectively.

The fiber reinforced laminated composite shell skin consists of a number of orthotropic layers having different orientations. For such a layer, the stress-strain relationship in the material axis system may be given by

$$\begin{Bmatrix} \sigma_1 \\ \sigma_2 \\ \tau_{12} \\ \tau_{23} \\ \tau_{31} \end{Bmatrix} = \begin{bmatrix} Q_{11} & Q_{12} & 0 & 0 & 0 \\ Q_{12} & Q_{22} & 0 & 0 & 0 \\ 0 & 0 & G_{12} & 0 & 0 \\ 0 & 0 & 0 & \beta_s G_{23} & 0 \\ 0 & 0 & 0 & 0 & \beta_s G_{31} \end{bmatrix} \begin{Bmatrix} \varepsilon_1 \\ \varepsilon_2 \\ \gamma_{12} \\ \gamma_{23} \\ \gamma_{31} \end{Bmatrix} \text{ or } \{\sigma\} = [Q]\{\varepsilon\} \tag{6}$$

where $Q_{11} = \frac{E_1}{1 - \nu_{12} \nu_{21}}$, $Q_{22} = \frac{E_2}{1 - \nu_{12} \nu_{21}}$, $Q_{12} = \frac{\nu_{21} E_1}{1 - \nu_{12} \nu_{21}} = \frac{\nu_{12} E_2}{1 - \nu_{12} \nu_{21}}$ and β_s is the shear correction

factor and it is taken as 5/6.

Though material axes 1-2 lie in x' - y' plane but it is oriented at an angle θ while axis 3 is directed along z' . With a simple coordinate transformation, the stress-strain relationship may be expressed in the local axis system $(x'$ - y' - $z')$ as follows.

$$\{\sigma'\} = [D']\{\varepsilon'\} \tag{7}$$

where $[D'] = [T_e]^T [Q] [T_e]$ and the transformation matrix $[T_e]$ can be expressed as

$$[T_e] = \begin{bmatrix} \cos^2 \theta & \sin^2 \theta & \sin \theta \cos \theta & 0 & 0 \\ \sin^2 \theta & \cos^2 \theta & -\sin \theta \cos \theta & 0 & 0 \\ -2 \sin \theta \cos \theta & 2 \sin \theta \cos \theta & \sin^2 \theta \cos^2 \theta & 0 & 0 \\ 0 & 0 & 0 & \cos \theta & \sin \theta \\ 0 & 0 & 0 & -\sin \theta & \cos \theta \end{bmatrix} \tag{8}$$

2.1.1 Elastic stiffness matrix

Once the matrices $[B]$ and $[D]$ are obtained, the elastic stiffness matrix of an element can be derived easily and it is expressed as

$$[k_e] = \int [B]^T [D'] [B] dx dy dz = \int [B]^T [D'] [B] |J| d\xi d\eta d\zeta \quad (9)$$

where $|J|$ is the determinant of the Jacobian matrix $[J]$, which can be obtained with the help of Eq. (1) taking derivatives of x , y and z with respect to ξ , η , and ζ .

The integration in Eq. (9) is carried out numerically following Gauss quadrature integration technique where two-point integration scheme has been adopted. The scheme is applied to all the layers in an element and their contributions are added together as follows.

$$[k_e] = \sum_{l=1}^{nl} \sum_{i=1}^2 \sum_{j=1}^2 \sum_{k=1}^2 [B(\xi_i, \eta_j, \zeta_k)]^T [D'_l] [B(\xi_i, \eta_j, \zeta_k)] |J(\xi_i, \eta_j, \zeta_k)| w_i w_j w_k \quad (10)$$

where nl is the number of layers in an element, $[D'_l]$ is the rigidity matrix $[D']$ as expressed in Eq. (7) of the l th layer, and w_i , w_j and w_k are the weight parameters. This technique is adopted in all the subsequent cases where integration is required to be carried out.

2.1.2 Mass matrix

The consistent mass matrix has been adopted in the present study. Following the usual techniques, it can be derived with the help of Eq. (1) and is expressed as

$$[m_e] = \int \rho [N_D]^T [N_D] dx dy dz = \int \rho [N_D]^T [N_D] |J| d\xi d\eta d\zeta \quad (11)$$

where ρ is the material density.

2.1.3 Geometric stiffness matrix

The geometric stiffness matrix may be obtained from the strain energy U_σ due to initial stress and it is expressed in terms of initial stress vector $\{\sigma'\}$ and nonlinear strain vector $\{\varepsilon_n'\}$ in the local axis system (x' - y' - z') as

$$U_\sigma = \frac{1}{2} \int [\sigma_{x'} \quad \sigma_{y'} \quad \tau_{x'y'} \quad \tau_{y'z'} \quad \tau_{z'x'}] \left\{ \begin{array}{l} \left(\frac{\partial u'}{\partial x'} \right)^2 + \left(\frac{\partial v'}{\partial x'} \right)^2 + \left(\frac{\partial w'}{\partial x'} \right)^2 \\ \left(\frac{\partial u'}{\partial y'} \right)^2 + \left(\frac{\partial v'}{\partial y'} \right)^2 + \left(\frac{\partial w'}{\partial y'} \right)^2 \\ \frac{\partial u'}{\partial x'} \frac{\partial u'}{\partial y'} + \frac{\partial v'}{\partial x'} \frac{\partial v'}{\partial y'} + \frac{\partial w'}{\partial x'} \frac{\partial w'}{\partial y'} \\ \frac{\partial u'}{\partial y'} \frac{\partial u'}{\partial z'} + \frac{\partial v'}{\partial y'} \frac{\partial v'}{\partial z'} + \frac{\partial w'}{\partial y'} \frac{\partial w'}{\partial z'} \\ \frac{\partial u'}{\partial z'} \frac{\partial u'}{\partial x'} + \frac{\partial v'}{\partial z'} \frac{\partial v'}{\partial x'} + \frac{\partial w'}{\partial z'} \frac{\partial w'}{\partial x'} \end{array} \right\} dv$$

Or

$$U_\sigma = \int \{\sigma'\}^T \{\varepsilon'_n\} dv \tag{12}$$

The above equation may be rewritten as

$$U_\sigma = \frac{1}{2} \int \{\varepsilon_g\}^T [\tau] \{\varepsilon_g\} dv \tag{13}$$

where

$$\{\varepsilon_g\} = \left[\frac{\partial u'}{\partial x'} \quad \frac{\partial u'}{\partial y'} \quad \frac{\partial u'}{\partial z'} \quad \frac{\partial v'}{\partial x'} \quad \frac{\partial v'}{\partial y'} \quad \frac{\partial v'}{\partial z'} \quad \frac{\partial w'}{\partial x'} \quad \frac{\partial w'}{\partial y'} \quad \frac{\partial w'}{\partial z'} \right]^T \tag{14}$$

and

$$[\tau] = \begin{bmatrix} [\tau^1] & 0 & 0 \\ 0 & [\tau^1] & 0 \\ 0 & 0 & [\tau^1] \end{bmatrix} \tag{15}$$

The sub matrix $[\tau^1]$ within the initial stress matrix $[\tau]$ in the above equation is

$$[\tau^1] = \begin{bmatrix} \sigma'_x & \tau'_{xy} & \tau'_{xz} \\ \tau'_{xy} & \sigma'_y & \tau'_{yz} \\ \tau'_{xz} & \tau'_{yz} & 0 \end{bmatrix} \tag{16}$$

Now the strain vector $\{\varepsilon_g\}$ in Eq. (14) may be expressed in terms of nodal displacement vector with the help of Eq. (2) as

$$\{\varepsilon_g\} = [B_g] \{\delta\} \tag{17}$$

With the help of above equation, the strain energy U_σ in Eq. (13) may be written as

$$U_\sigma = \frac{1}{2} \{\delta\}^T [k_g] \{\delta\} \tag{18}$$

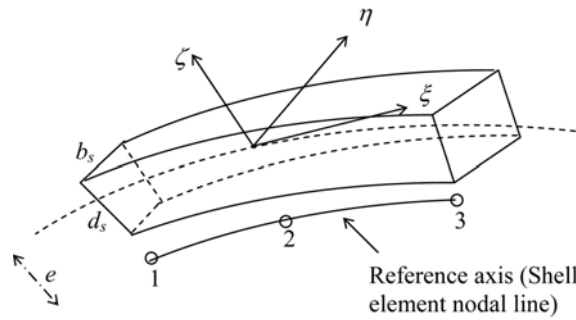


Fig. 3 Degenerated curved beam element

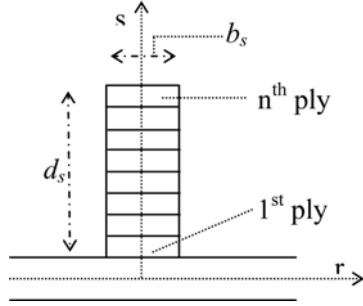


Fig. 4(a) Ply arrangement I (parallel)

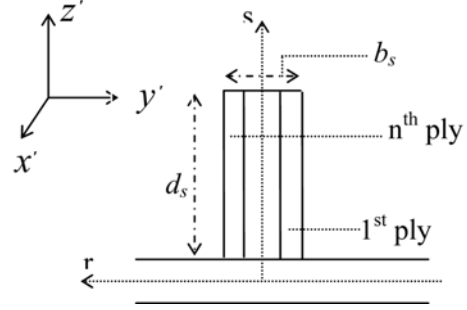


Fig. 4(b) Ply arrangement II (perpendicular)

where $[k_g]$ is the geometric stiffness matrix and it may be expressed as

$$[k_g] = \int [B_G]^T [\tau] [B_G] dv = \int [B_G]^T [\tau] [B_G] |J| d\xi d\eta d\zeta \quad (19)$$

2.2 Stiffener element

The derivation of the stiffener element (Fig. 3) is based on the basic concept used to derive the shell element. In this case the stiffener element modeled with three dimensional solid element is degenerated with the help of certain extractions obtained from the consideration that the dimension across stiffener depth as well as breadth is small compared to that along the length. The stiffener element follows an edge of a shell element where the parameters of three nodes lying on that shell element edge are used to express the geometry and deformation of the stiffener utilizing compatibility between shell and stiffeners (Fig. 4). It helps to eliminate the involvement of additional degrees of freedom for the modeling of stiffeners. The stiffener element having any arbitrary curved geometry is mapped into a regular domain in ξ - η - ζ coordinate system where all these coordinates vary from -1 to $+1$. Again ξ is taken along the stiffener axis while η and ζ are taken along the width and depth directions respectively. It has been found that the vectors \bar{v}_{1i} , \bar{v}_{2i} and \bar{v}_{3i} are quite useful for the representation of geometry and deformation of the shell element. For the stiffener element a similar set of vectors \bar{v}_{1i}^s , \bar{v}_{2i}^s and \bar{v}_{3i}^s are used and these may be obtained from those of the shell element (\bar{v}_{1i} , \bar{v}_{2i} and \bar{v}_{3i}) as

$$\bar{v}_1^s = \bar{v}_1 \cos \theta_s + \bar{v}_2 \sin \theta_s, \quad \bar{v}_2^s = -\bar{v}_1 \sin \theta_s + \bar{v}_2 \cos \theta_s \quad \text{and} \quad \bar{v}_3^s = \bar{v}_3 \quad (20)$$

where $(\bar{v}_{1i}^s - \bar{v}_{2i}^s)$ is oriented at an angle of θ_s with respect to $(\bar{v}_{1i} - \bar{v}_{2i})$ and \bar{v}_{1i}^s follows the stiffener axis.

With these vectors, the coordinate at any point within the stiffener may be expressed in terms of coordinates (x_i, y_i, z_i) of those three nodes of the corresponding shell element edge as

$$\begin{Bmatrix} x \\ y \\ z \end{Bmatrix} = \sum_{i=1}^3 N_{si} \begin{Bmatrix} x_i \\ y_i \\ z_i \end{Bmatrix} + \sum_{i=1}^3 N_{si} \left(\frac{\zeta d_s}{2} + e \right) \begin{Bmatrix} l_{3i}^s \\ m_{3i}^s \\ n_{3i}^s \end{Bmatrix} + \sum_{i=1}^3 N_{si} \left(\frac{\eta b_s}{2} \right) \begin{Bmatrix} l_{2i}^s \\ m_{2i}^s \\ n_{2i}^s \end{Bmatrix} \quad (21)$$

where b_s is stiffener width, d_s is its depth and e is the eccentricity (distance of the stiffener axis

from the shell mid surface). The expressions of the quadratic shape functions N_{si} along ξ are as follows.

$$N_{s1} = \xi(\xi - 1)/2, \quad N_{s2} = 1 - \xi^2, \quad N_{s3} = \xi(\xi + 1)/2$$

Now considering the deformation of the stiffener element, the present formulation differs from the usual one (Bathe 1996, Ferguson and Clark 1979, Liao and Reddy 1990) where six degrees of freedom are generally taken to represent the biaxial bending apart from torsion and axial deformation. In the present study the bending of the stiffener in the tangential plane of the shell is not considered. This has helped to eliminate the involvement the sixth degrees of freedom θ_z like that of shell element. Moreover the usual formulation (Bathe 1996, Ferguson and Clark 1979, Liao and Reddy 1990) overestimates the torsional rigidity and it cannot be corrected simply with some correction factor since it got mixed with other terms. The present formulation facilitates to treat it nicely where a torsion correction factor is introduced for parallel as well as perpendicular stacking schemes. Actually this is the primary object for the reformulation of the stiffener element. Based on this the displacement components at any point within the stiffener may be expressed as

$$\begin{Bmatrix} u \\ v \\ w \end{Bmatrix} = \sum_{i=1}^3 N_{si} [T_{vi}] \begin{Bmatrix} u_i \\ v_i \\ w_i \end{Bmatrix} - \sum_{i=1}^3 N_{si} \left(\frac{\xi d_s}{2} + e \right) \begin{bmatrix} l_{1i} & l_{2i} \\ m_{1i} & m_{2i} \\ n_{1i} & n_{2i} \end{bmatrix} \begin{Bmatrix} \theta_{xi} \\ \theta_{yi} \end{Bmatrix} = [N_{Ds}] \{ \delta_s \} \quad (22)$$

where $\{ \delta_s \} = [u_1 \ v_1 \ w_1 \ \theta_{x1} \ \theta_{y1} \ u_2 \ v_2 \ \dots \ \theta_{y3}]^T$ and l_1, m_1 and n_1 are the direction cosine of the vectors $\bar{v}_{1i}^s, \bar{v}_{2i}^s$ and \bar{v}_{3i}^s with respect to the global coordinates (x, y and z), the matrix $[T_{vi}]$ is used to make the component of translational displacement along \bar{v}_{2i}^s at shell mid-plane zero since the bending of the stiffener in the tangential plane of the shell is not considered. Its effect should be insignificant since bending deformation in this mode will be very small due to high in-plane rigidity of the shell skin. Moreover the flexural rigidity of stiffener in this mode is usually found to be small.

The matrix $[T_{vi}]$ used in the above equation may be expressed with the help of $\bar{v}_{1i}^s, \bar{v}_{2i}^s$ as

$$[T_{vi}] = \begin{bmatrix} l_{1i}^s & 0 & l_{3i}^s \\ m_{1i}^s & 0 & m_{3i}^s \\ n_{1i}^s & 0 & n_{3i}^s \end{bmatrix} \begin{bmatrix} l_{1i}^s & m_{1i}^s & n_{1i}^s \\ l_{2i}^s & m_{2i}^s & n_{2i}^s \\ l_{3i}^s & m_{3i}^s & n_{3i}^s \end{bmatrix} \quad (23)$$

Similar to shell element, the stress and strain components at any point within the stiffener element are taken in a local axis system ($x'-y'-z'$) corresponding to $\bar{v}_{1i}^s, \bar{v}_{2i}^s$ and \bar{v}_{3i}^s . The relationship between them may be expressed as

$$\begin{Bmatrix} \sigma_{x'} \\ \tau_{x'z'} \\ \tau_{x'y'} \end{Bmatrix} = \begin{bmatrix} \bar{Q}_{1m} & 0 & 0 \\ 0 & \beta_s \bar{Q}_{5m} & 0 \\ 0 & 0 & \beta_t \bar{Q}_{6m} \end{bmatrix} \begin{Bmatrix} \epsilon_{x'} \\ \gamma_{x'z'} \\ \gamma_{x'y'} \end{Bmatrix} \text{ or } \{ \sigma' \} = [D'_s] \{ \epsilon' \} \quad (24)$$

where β_s is the shear correction factor, which is taken as 5/6. The torsion correction factor β_t and

other rigidity parameters in the rigidity matrix $[D'_s]$ are presented below for two different types of stacking arrangements of the stiffener as shown in Fig. 4. For both the arrangements, the stress-strain relationship of a lamina in its axis system ($x'r-s$) as shown in Fig. 4 may be written as

$$\begin{Bmatrix} \sigma_{x'} \\ \sigma_r \\ \tau_{x'r} \\ \tau_{x's} \\ \tau_{rs} \end{Bmatrix} = \begin{bmatrix} \bar{Q}_{11} & \bar{Q}_{12} & \bar{Q}_{16} & 0 & 0 \\ \bar{Q}_{21} & \bar{Q}_{22} & \bar{Q}_{26} & 0 & 0 \\ \bar{Q}_{61} & \bar{Q}_{62} & \bar{Q}_{66} & 0 & 0 \\ 0 & 0 & 0 & \bar{Q}_{55} & \bar{Q}_{54} \\ 0 & 0 & 0 & \bar{Q}_{45} & \bar{Q}_{44} \end{bmatrix} \begin{Bmatrix} \varepsilon_{x'} \\ \varepsilon_r \\ \gamma_{x'r} \\ \gamma_{x's} \\ \gamma_{rs} \end{Bmatrix} \quad (25)$$

where the rigidity matrix in the above equation is identical to $[D']$ of the shell element obtained in Eq. (5).

The rigidity parameters $[D'_s]$ of Eq. (24) may be obtained from Eq. (25), utilizing the conditions ($\sigma_r = 0$) and ($\tau_{rs} = 0$). For ply arrangement I, the rigidity parameters will be

$$\begin{aligned} \bar{Q}_{1m} &= \bar{Q}_{11} + \bar{Q}_{12} \frac{\bar{Q}_{61}\bar{Q}_{26} - \bar{Q}_{21}\bar{Q}_{66}}{\bar{Q}_{22}\bar{Q}_{66} - \bar{Q}_{62}\bar{Q}_{26}} + \bar{Q}_{16} \frac{\bar{Q}_{61}\bar{Q}_{22} - \bar{Q}_{21}\bar{Q}_{62}}{\bar{Q}_{26}\bar{Q}_{62} - \bar{Q}_{66}\bar{Q}_{22}} \\ \bar{Q}_{5m} &= \bar{Q}_{55} - \bar{Q}_{54} \frac{\bar{Q}_{45}}{\bar{Q}_{44}} \text{ and } \bar{Q}_{6m} = \bar{Q}_{66} \end{aligned}$$

For ply arrangement II, the rigidity parameters are as follows.

$$\begin{aligned} \bar{Q}_{1m} &= \bar{Q}_{11} + \bar{Q}_{12} \frac{\bar{Q}_{61}\bar{Q}_{26} - \bar{Q}_{21}\bar{Q}_{66}}{\bar{Q}_{22}\bar{Q}_{66} - \bar{Q}_{62}\bar{Q}_{26}} + \bar{Q}_{16} \frac{\bar{Q}_{61}\bar{Q}_{22} - \bar{Q}_{21}\bar{Q}_{62}}{\bar{Q}_{26}\bar{Q}_{62} - \bar{Q}_{66}\bar{Q}_{22}} \\ \bar{Q}_{5m} &= \bar{Q}_{66} \text{ and } \bar{Q}_{6m} = \bar{Q}_{55} - \bar{Q}_{54} \frac{\bar{Q}_{45}}{\bar{Q}_{44}} \end{aligned}$$

The torsion correction factor β_i for these two cases may be written as

$$\begin{aligned} \text{Ply arrangement I: } \beta_i &= \frac{3kb_s^2 \sum_{i=1}^{nls} \bar{Q}_{5m}^i (s_{i+1} - s_i)}{\sum_{i=1}^{nls} \bar{Q}_{6m}^i (s_{i+1}^3 - s_i^3)} \\ \text{Ply arrangement II: } \beta_i &= \frac{12kd_s \sum_{i=1}^{nls} \bar{Q}_{5m}^i (s_{i+1}^3 - s_i^3)}{[(d_s + h/2)^3 - (h/2)^3] \sum_{i=1}^{nls} \bar{Q}_{6m}^i (s_{i+1} - s_i)} \end{aligned}$$

where nls is the number of layers of the stiffener rib and k is the factor to get torsion constant of an isotropic beam having rectangular section, which is a function of b_s/d_s ratio of the rectangular section (Timoshenko and Goodier 1951).

Now Eqs. (20)-(24) may be used to derive the elastic stiffness matrix $[k_{es}]$, mass matrix $[m_{es}]$ and geometric stiffness matrix $[k_{gs}]$ of a stiffener element following the procedure used for shell element and these matrices may be expressed as follows.

$$[k_{es}] = \int [B_s]^T [D'_s] [B_s] dx dy dz = \int [B_s]^T [D'_s] [B_s] |J| d\xi d\eta d\zeta \quad (26)$$

$$[m_{es}] = \int \rho [N_{Ds}]^T [N_{Ds}] dx dy dz = \int \rho [N_{Ds}]^T [N_{Ds}] |J| d\xi d\eta d\zeta \quad (27)$$

$$[k_{gs}] = \int [B_{Gs}]^T [\tau] [B_{Gs}] dx dy dz = \int [B_{Gs}]^T [\tau] [B_{Gs}] |J| d\xi d\eta d\zeta \quad (28)$$

where $[B_s]$ and $[B_{Gs}]$ are analogous to $[B]$ and $[B_G]$ respectively. The initial stress matrix $[\tau]$ looks identical to that of shell (15) but its sub matrix $[\tau^1]$ for stiffener element is

$$[\tau^1] = \begin{bmatrix} \sigma'_x & 0 & 0 \\ 0 & 0 & 0 \\ 0 & 0 & 0 \end{bmatrix} \quad (29)$$

The elastic stiffness matrix, mass matrix and geometric stiffness matrix are computed for all the shell elements and stiffener elements of the entire structure and these matrices are accordingly assembled together to form the corresponding global matrices $[K]$, $[M]$ and $[K_G]$ where the skyline storage algorithm is used to keep these three big size matrices in single array.

2.3 Governing equations

With the stiffness matrix $[K]$, mass matrix $[M]$ and geometric stiffness matrix $[K_G]$ of the structure obtained in the previous section, the equation of motion of the structure can be written as

$$[M]\{\ddot{q}\} + [[K] - P[K_G]]\{q\} = \{0\} \quad (30)$$

This is a general equation and it can be reduced as a special case to get the governing equations for buckling, vibration and dynamic stability problems as follows.

2.3.1 Buckling

$$[[K] - P_{cr}[K_G]]\{q\} = \{0\} \quad (31)$$

where P_{cr} is the critical load of buckling.

2.3.2 Vibration

$$[[K] - P[K_G]]\{q\} - \omega^2[M]\{q\} = \{0\} \quad (32)$$

where ω is the vibration frequency of the structure subjected to in-plane load and it becomes the natural frequency of vibration if P is made zero.

2.3.3 Dynamic stability

Eq. (30) can also be used to solve the dynamic stability problem. Let the in-plane load P be periodic and may be expressed as

$$P(t) = P_s + P_l \cos \Omega t \quad (33)$$

where Ω is the frequency of excitation, P_s is the static component of P and P_l is the amplitude of its dynamic component, which may be expressed in terms of static buckling load P_{cr} as follows.

$$P_s = \alpha P_{cr}, P_l = \beta P_{cr} \quad (34)$$

where α and β may be defined as static and dynamic load factors respectively. Now Eq. (30) can be written as

$$[M]\{\ddot{q}\} + [[K] - \alpha P_{cr}[K_G] - \beta P_{cr}[K_G] \cos \Omega t]\{q\} = 0 \quad (35)$$

The above equation represents a system of second order differential equation with periodic coefficient, which is basically the Mathieu-Hill equation. The boundaries of dynamic instability regions can be found by the periodic solutions having period of T and $2T$, where $T = 2\pi/\Omega$. The range of primary instability region with period of $2T$ is of practical importance (Bolotin 1964) where the solution can be achieved by expressing $\{q\}$ in the form of the trigonometric series as

$$\{q\} = \sum_{k=1,3,5}^{\infty} \left[\{a_k\} \sin \frac{k\Omega t}{2} + \{b_k\} \cos \frac{k\Omega t}{2} \right] \quad (36)$$

After substitution of the above equation in Eq. (31) and taking the first term of the series, the quantities associated with $\sin \Omega t/2$ and $\cos \Omega t/2$ are separated out and processed accordingly to eliminate the time dependent component and it leads to

$$\left[[K] - \alpha P_{cr}[K_G] \pm \frac{1}{2} \beta P_{cr}[K_G] - \frac{\Omega^2}{4} [M] \right] \{q_{ab}\} = 0 \quad (37)$$

where $\{q_{ab}\}$ is either $\{a_k\}$ or $\{b_k\}$ depending on the use of plus or minus of the dynamic in-plane load component respectively. It is basically an eigenvalue problem and it can be solved for known value of α , β and P_{cr} . The two frequencies corresponding to plus and minus will indicate the boundaries of the dynamic instability region.

3. Results and discussions

The convergence and validation of the proposed model is presented taking various examples from the literature. The proposed study is presented with problem definition, free vibration, buckling and dynamic instability analysis of the stiffened shell panels.

3.1 Convergence and validation

The convergence and accuracy of the proposed method are first established by comparing the results of various problems with those of earlier investigators' available in the literature.

Table 1 Non-dimensional bounding frequency ($\bar{\Omega}$) for un-stiffened simply supported square plate

Analysis	Non-dimensional bounding frequency ($\bar{\Omega}$)			
	$\alpha = 0.0$ and $\beta = 0.8$		$\alpha = 0.6$ and $\beta = 0.32$	
	L ^a	U ^b	L ^a	U ^b
Present (2 × 2)	50.82	77.27	32.22	49.11
Present (4 × 4)	30.80	47.06	19.48	29.76
Present (6 × 6)	30.58	46.71	19.34	29.54
Present (8 × 8)	30.57	46.69	19.33	29.53
Present (10 × 10)	30.56	46.69	19.33	29.53
Present (12 × 12)	30.56	46.69	19.33	29.53
Present (14 × 14)	30.56	46.69	19.33	29.53
Present (16 × 16)	30.56	46.69	19.33	29.53
Present (18 × 18)	30.56	46.69	19.33	29.53
Hutt and Salam (1971)	30.57	46.69	19.53	29.60
Srivastava <i>et al.</i> (2002)	30.57	46.71	19.33	29.54

^aLower boundary of the instability zone

^bUpper boundary of the instability zone

3.1.1 Dynamic instability of un-stiffened simply supported square plate

The problem of un-stiffened simply supported square plate ($a \times a$) is used to carry out the convergence study. The a/h ratio of the plate is 100. The plate is subjected to uniform loading in the two opposite edges. The whole structure is modeled with a number of mesh sizes to carry out the analysis. The non-dimensional ($\bar{\Omega} = \Omega b^2 \sqrt{\rho h/D}$) lower and upper bounding excitation frequencies of the dynamic instability zones are shown in Table 1 for two sets of α and β values for all the mesh sizes. It shows a rapid convergence with mesh refinement. Again a mesh size of 8×8 is found to be sufficient to attain the convergence and this is used for all the subsequent analyses. For validation, the results are compared with those of Hutt and Salam (1971), Srivastava *et al.* (2002). The results obtained in these studies (Hutt and Salam 1971, Srivastava *et al.* 2002) are found to be in good agreement compared to present results.

3.1.2 Free vibration of a spherical shell panel of square base having two stiffeners along its two centerlines

The stiffened spherical shell panel as shown in Fig. 5 is also used to carry out the convergence study taking its four sides as simply supported (SSSS) as well as clamped (CCCC) conditions. The simply supported boundary condition in the two edges is shown in the Fig. 5. The top and bottom side have same boundary condition. Similarly the left and right side have same boundary condition. The details of the shell and stiffeners are given in Fig. 5 where the stiffeners are taken to be symmetric with respect to the shell mid surface. Similar to the previous problem the structure is modeled with a number of mesh sizes to carry out the analysis. The first two natural frequencies for both the boundary conditions are plotted in Fig. 6. It is observed that with mesh refinement the results are converging rapidly. Here also a mesh size of 8×8 is found to be sufficient to attain the convergence. To validate the results, the first five frequencies (mesh size 8×8) for the simply supported boundary condition are compared with the results of finite element solution of Nayak and

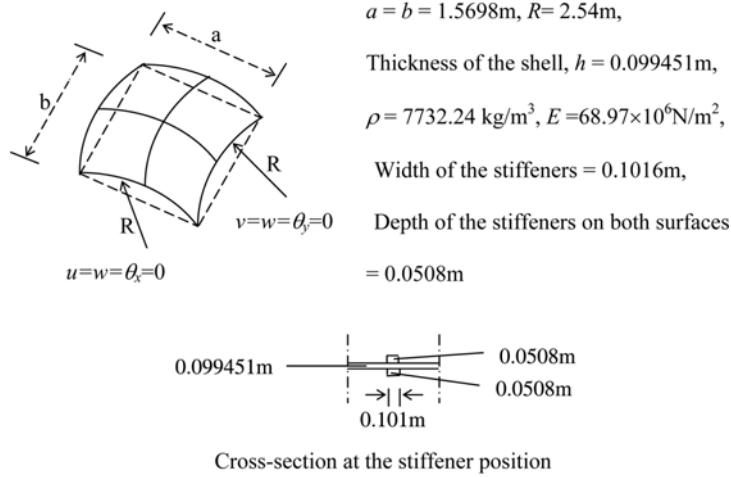
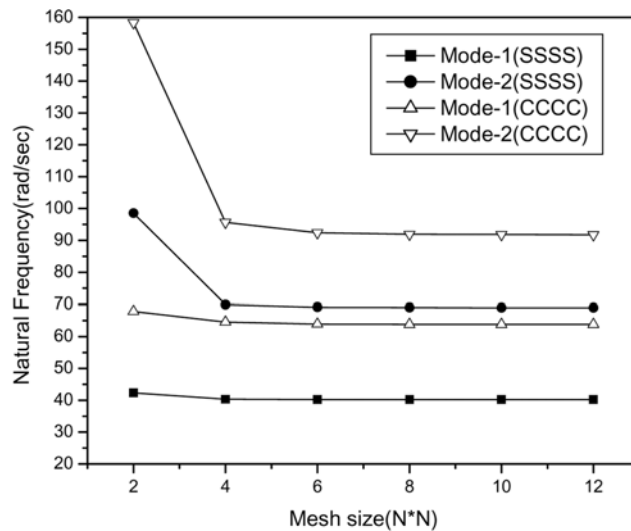


Fig. 5 Stiffened spherical shell panel having square base



(The mesh size is considered taking the full structure)

Fig. 6 Convergence for frequency of vibration with mesh size of a stiffened spherical shell panel having square base

Bandopadhyay (2002), Samanta and Mukhopadhyay (2004), Prusty (2001) in Table 2. The results are found to be in good agreement.

3.1.3 Free vibration of a rectangular composite stiffened plate

The laminated (0/90/0) rectangular plate with three unidirectional laminated (0/90/0) stiffeners as shown in Fig. 7 is analyzed taking simply supported boundary condition at the four sides. The detail of geometry and material properties are given in Fig. 7. The frequencies for first five modes

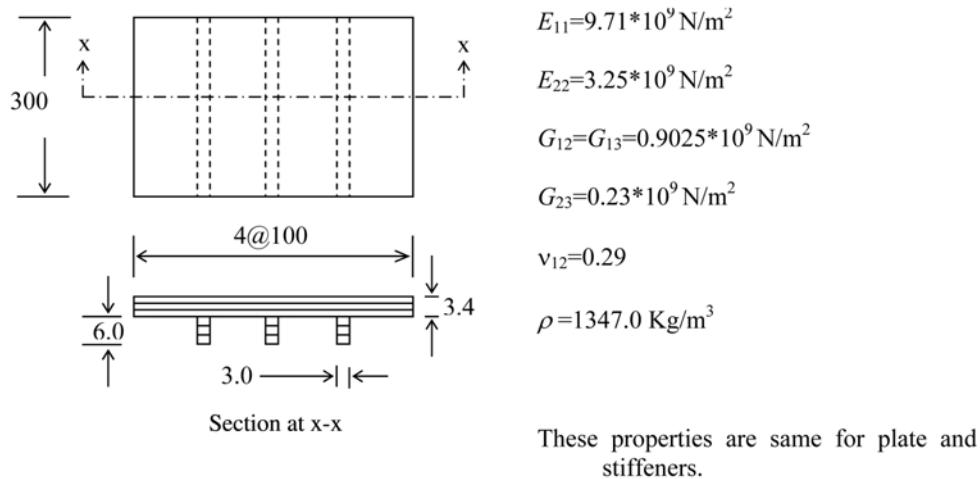
Table 2 Natural frequency (rad/sec) of simply supported spherical shell panel with two stiffeners along the two central lines

Mode Number	Present (8×8)	Nayak and Bandopadhyay (2002)		Samanta and Mukhopadhyay (2004) (8 × 8)	Prusty (2001) (16 × 16)
		EI-8 ^a (8 × 8)	EI-9 ^b (8 × 8)		
1	40.2300	40.26	40.26	41.70	40.81
2	69.0282	70.98	70.97	74.11	72.13
3	69.1158	70.98	70.97	74.36	72.13
4	91.2984	96.06	96.06	99.18	92.92
5	105.6800			104.94	105.69

(The mesh size is considered taking the full structure in all cases)

^aEight noded element

^bNine noded element



All dimensions are in mm

Fig. 7 Simply supported laminated plate with three unidirectional laminated stiffeners

Table 3 Natural frequencies (Hz) of a simply supported stiffened composite plate

References	Mode 1	Mode 2	Mode 3	Mode 4	Mode 5
Present	65.216	98.643	168.36	231.96	255.64
Chao and Lee (1980)	65.000	101.00		228.00	260.00
Prusty (2001)	63.510	95.840	162.97	223.09	245.37
Chattopadhyay <i>et al.</i> (1992)	63.000	95.000		225.00	250.00

obtained in the present analysis are presented in Table 3 with some other finite element results reported by Prusty (2001), Chao and Lee (1980), Chattopadhyay *et al.* (1992). The table shows that the results agreed well.

3.1.4 Free vibration of a composite stiffened spherical shell panel of square base

The laminated spherical shell panel having two laminated central stiffeners (Fig. 8) placed inside the shell surface is analyzed taking stacking sequence for the shell and the stiffener as 0/90/0/90 in one case (I) and 45/-45/45/-45 in other case (II). Fig. 8 shows all the details of the composite stiffened shell panel. The numbering of layers starts from bottom to top both in stiffener and panel skin. The analysis is carried out for three different values of curvature ratio (R/a) taking simply supported boundaries at the four edges. The fundamental frequencies obtained in the present analysis are presented with finite element solution of Prusty (2001) in Table 4, which shows that the results are in good agreement.

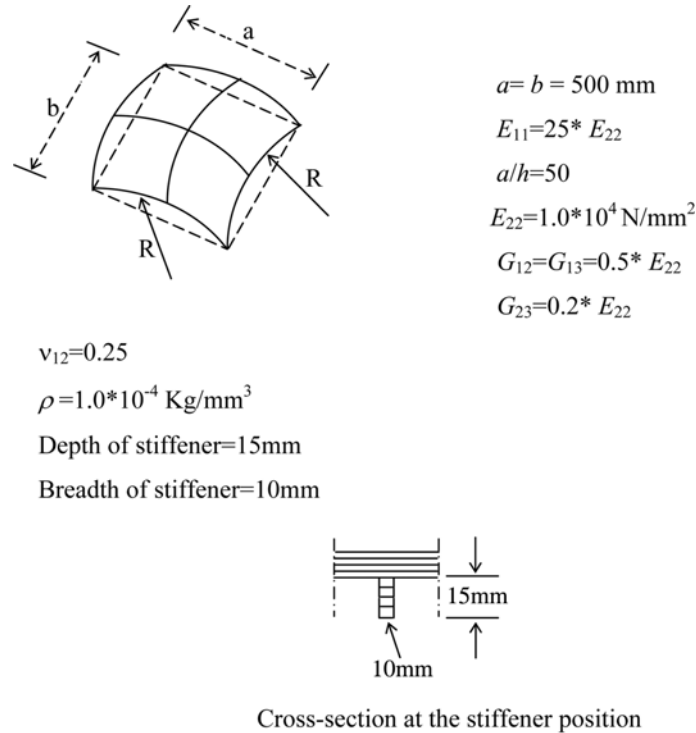


Fig. 8 Laminated spherical shell panel with two central laminated stiffeners attached to the bottom surface

Table 4 Natural frequencies (Hz) of a laminated composite spherical shell panel with two central laminated stiffeners attached to the bottom surface

Lamination	References	$R/a = 5$	$R/a = 10$	$R/a = 100$
Case – I	Present	1.415	1.239	1.183
	Prusty (2001)	1.410	1.238	1.183
Case – II	Present	2.426	1.596	1.207
	Prusty (2001)	2.446	1.682	1.358

Table 5 Buckling load parameter (k) for a simply supported rectangular stiffened plate under uniaxial compression

a/b	$\gamma = 10, \delta = 0.05$			$\gamma = 5, \delta = 0.2$		
	Present	Timoshenko and Gere (1961)	Mukhopadhyay (1989)	Present	Timoshenko and Gere (1961)	Mukhopadhyay (1989)
0.6	16.403	16.5		16.463	16.5	
0.8	16.686	16.8		12.729	13.0	
1.0	15.908	16.0	15.91	9.612	9.72	9.65
2.0	10.110	10.2	10.16	6.244	6.24	6.24
3.0	11.867	12.0	11.94	6.512	6.53	6.48
4.0	10.135	10.2		6.264	6.24	

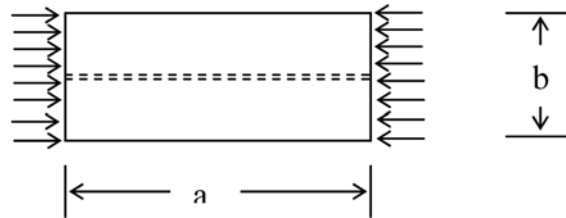


Fig. 9 Simply supported stiffened rectangular plate under uniaxial compression

3.1.5 Buckling of a rectangular plate with a central stiffener under uniaxial load

The problem of the rectangular stiffened plate (Fig. 9) having simply supported boundary conditions at its four edges is investigated for different plate aspect ratio (a/b) and stiffener parameters ($\delta = A_s/bh, \gamma = EI_s/bD$ where A_s - cross-sectional area of the stiffener, I_s - moment of inertia of the stiffener). The simply supported boundary condition is as SSSS in section 3.1.2. The plate thickness ratio (a/h) and isotropic plate and stiffener material (ν) are taken as 100 and 0.3 respectively. The dimension a is varied keeping b as constant to get different values of aspect ratio (a/b). The non-dimensional critical buckling stress parameter $k = \sigma_{cr}/(\pi^2 D/b^2 h)$ obtained in the present analysis is presented in Table 5 with the analytical solution of Timoshenko and Gere (1961) and finite element solution of Mukhopadhyay (1989). The table shows that the agreement between the results is very good. As Timoshenko and Gere (1961) have not considered the effect of stiffener eccentricity and torsional rigidity, these parameters are taken as zero in the present problem.

3.1.6 Buckling of a laminated cylindrical shell panel under axial compression

The laminated (0/90/0/90/0) cylindrical shell panel of square base ($a \times a$) simply supported along all four edges is analyzed taking curvature ratio $R/a = 20$ and thickness ratio $a/h = 10, 20, 30, 50$ and 100. The values of non-dimensional buckling load parameter $\bar{N}_{cr} = N_{cr} a^2 / E_{22} h^3$ obtained in the present analysis are presented with those of Sciuva and Crrera (1990) Table 6, which shows that the results agreed well. The material properties used are: $E_{11} = 40E_{22}, G_{12} = G_{13} = 0.5E_{22}, G_{23} = 0.6E_{22}$ and $\nu_{12} = 0.25$.

Table 6 Non-dimensional buckling load parameter of a simply supported cross-ply cylindrical shell panel under axial compression

References	a/h				
	10	20	30	50	100
Present	23.964	31.792	33.981	35.395	36.845
Sciuva and Crrera (1990)	24.19	31.91	34.04	35.42	36.86

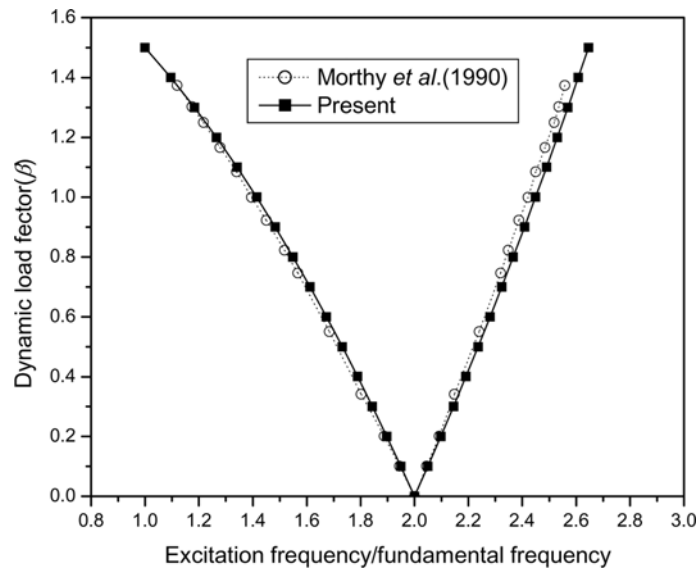


Fig. 10 Comparison of upper and lower bounding frequencies for a simply supported laminated composite square plate

3.1.7 Dynamic instability of a laminated composite square plate simply supported at the four sides

The simply supported laminated square plate ($a \times a$), (standard case, Moorthy *et al.* 1990) with four layer, symmetric cross-ply (0/90/90/0) laminates under in-plane pulsating load along the direction of 0 degree laminate is analyzed for different values of dynamic load factor β taking static load factor α to be zero. The plate parameters are, $a = 0.254$ m, $a/h = 25$, $\rho = 2.7712 \times 10^{10}$ kg/m³, $E_{22} = 6.8982 \times 10^{10}$ N/m², $E_{11}/E_{22} = 40.0$, $G_{12} = G_{13} = 0.6E_{22}$, $G_{23} = 0.5E_{22}$ and $\nu_{12} = 0.25$. The values of bounding frequencies obtained in the present analysis are plotted with those of Moorthy *et al.* (1990) in Fig. 10, which shows that the agreement between the results is very good.

3.2 Proposed study

In the proposed study the free vibration, buckling and dynamic instability analyses are carried out for a laminated stiffened shell problem where its different parameters are varied in a wide range to study the effect of these parameters on the behavior of the structure. The detail is given below.

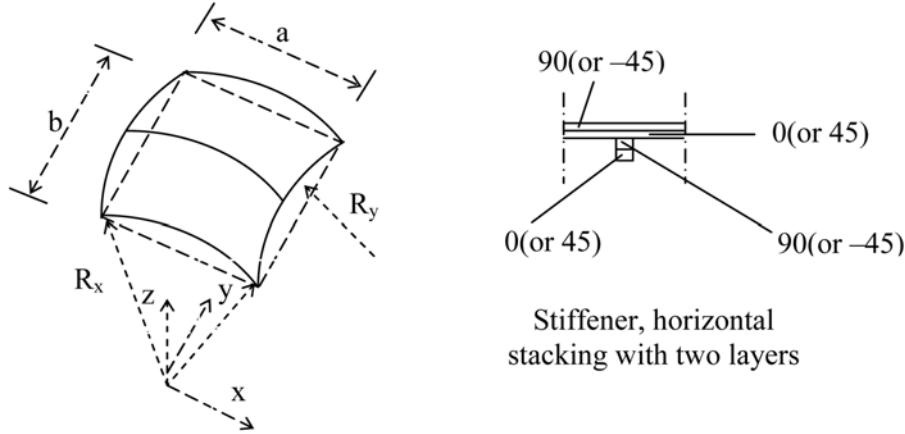


Fig. 11 A doubly curved laminated shell panel with a central laminated stiffener (xst)_b

3.2.1 Problem definition

It is a doubly curved laminated shell panel having laminated stiffeners subjected to uniform pressure along x -direction. Fig. 11 shows the panel with a central stiffener. The radii of curvatures are taken in such a manner to get some specific geometry such as flat plate ($a/R_x = 0.0$, $b/R_y = 0.0$), cylindrical shell panel ($a/R_x = 0.0$, $b/R_y = 0.5$), spherical shell panel ($a/R_x = 0.5$, $b/R_y = 0.5$) and hyperbolic hyperboloid ($a/R_x = -0.5$, $b/R_y = 0.5$). The lamination scheme for the shell and the stiffener adopted is (0/90/0/90/---) in one case and (45/-45/45/-45/---) in the other case. The number of layers in the skin of shell panel and stiffener are taken to be same in all the cases. However this is varied from two to eight layers. For the stiffener, parallel stacking scheme is adopted except the case in which the effect of stacking scheme is considered. In many cases the depth to width ratio (d_s/b_s) of the stiffener is varied where the stiffener width is always taken as the shell thickness (h). Moreover the thickness ratio (a/h) and aspect ratio (a/b) taken are 100 and 1 respectively in all the cases. The stiffener is placed at the inner surface of the shell panel except the case in which the effect of eccentricity is considered. The terminology for stiffeners for bottom and top positions are as (xst)_b-stiffener in x -direction in bottom surface, (xst)_t-stiffener in x -direction in top surface, (yst)_b-stiffener in y -direction in bottom surface and (yst)_t-stiffener in y -direction in top surface. In all the cases the four sides of the shell panel are taken to be simply supported and the material properties used for shell as well as stiffener are $E_{11} = 40E_{22}$, $G_{12} = G_{13} = 0.6E_{22}$, $G_{23} = 0.5E_{22}$, $\nu_{12} = 0.25$.

The results obtained in three types of analyses mentioned above are presented in non-dimensional form as follows.

$$\text{Non-dimensional natural frequency: } \bar{\omega} = \omega b^2 \sqrt{\rho/E_{22}h^2}$$

$$\text{Non-dimensional buckling load: } \bar{N}_x = N_x b^2/E_{22}h^3$$

$$\text{Non-dimensional bounding excitation frequency: } \bar{\Omega} = \Omega b^2 \sqrt{\rho/E_{22}h^2}$$

3.2.2 Free vibration

The free vibration analysis is carried out for 2, 4, 6 and 8 layer configurations taking (d_s/b_s) ratios of the stiffener as 2, 4, 6 and 8. The results obtained are presented in Table 7 and Table 8 for cross-ply and angle-ply stacking respectively.

Table 7 Non-dimensional fundamental frequency of cross-ply laminated shell panel with cross-ply laminated stiffener

Shell panel/ stiffener lamination	d_s/b_s	Flat plate	Cylindrical panel	Spherical panel	Hyperbolic hyperboloid panel
(0/90) ₁	2	17.276	35.960	74.401	16.814
	4	28.686	35.928	77.189	28.690
	6	31.461	35.831	82.138	38.773
	8	31.358	35.464	86.019	44.199
(0/90) ₂	2	21.434	42.349	75.445	20.955
	4	32.096	47.857	77.837	31.249
	6	42.422	51.492	82.538	41.730
	8	48.882	51.208	87.871	50.341
(0/90) ₃	2	22.042	42.656	75.617	21.569
	4	32.253	47.952	77.849	31.394
	6	42.605	53.887	82.397	41.759
	8	50.738	53.590	87.703	50.493
(0/90) ₄	2	22.231	42.754	75.671	21.762
	4	32.220	47.929	77.817	31.362
	6	42.537	54.705	82.277	41.648
	8	50.782	54.404	87.551	50.416

Table 8 Non-dimensional fundamental frequency of angle-ply laminated shell panel with angle-ply laminated stiffener

Shell panel/ stiffener lamination	d_s/b_s	Flat plate	Cylindrical panel	Spherical panel	Hyperbolic hyperboloid panel
(45/-45) ₁	2	18.456	41.394	108.622	18.601
	4	19.973	41.351	106.707	19.864
	6	22.973	41.224	104.405	22.359
	8	26.972	40.992	102.137	25.697
(45/-45) ₂	2	24.221	57.729	123.078	23.788
	4	25.069	57.639	122.770	24.558
	6	27.303	57.442	122.130	26.544
	8	30.754	57.101	121.022	29.555
(45/-45) ₃	2	24.952	60.229	124.354	24.470
	4	25.743	60.132	124.017	25.188
	6	27.892	59.925	124.372	27.108
	8	31.265	59.569	122.274	30.065
(45/-45) ₄	2	25.196	61.080	124.795	24.698
	4	25.969	60.981	124.449	25.400
	6	28.091	60.771	124.801	27.298
	8	31.437	60.409	122.706	30.236

It is observed that the ply orientation has effect on vibration characteristics of the structure. The frequency of angle-ply orientation is found to be more compared to that of cross-ply scheme for cylindrical and spherical panels. But for flat and hyperbolic hyperboloid panels the frequency of

angle-ply orientation is less compared to that of cross-ply scheme for d_s/b_s equals to 4, 6 and 8. Again the frequency of cylindrical and spherical panels is always more than that of flat plate and this is due to the fact that the curvature introduces additional stiffening effect. This situation in hyperbolic hyperboloid is different since the curvatures in the two principal directions are opposite in nature. In case of cross-ply lamination scheme, the frequency is found to be always increasing with the increase of stiffener depth except $(0/90)_1$ in flat and cylindrical panel. In angle-ply stacking sequence the frequency is increasing with increase in stiffener depth for flat and hyperbolic hyperboloid panel, but in case of cylindrical and spherical panels the frequency is increasing with the increase in stiffener depth up to certain depth and after that the frequency is dropping down. With the increase in the number of layers the frequencies values are increasing in all the cases.

3.2.3 Buckling

Similar to the vibration analysis presented above, the buckling analysis is carried out in this section and the results obtained in the form of non-dimensional buckling load parameters are presented in Table 9 and Table 10 for cross-ply and angle-ply stacking respectively. It is observed that the non-dimensional buckling loads of flat plate and hyperbolic hyperboloid panel for $(45/-45)_n$ and $d_s/b_s = 2$ is more compared to that of $(0/90)_n$ and $d_s/b_s = 2$. For cylindrical shell panel the buckling loads are more in case of angle-ply lamination compared to cross-ply lamination scheme. In spherical shell panel the non-dimensional buckling load for $(45/-45)_n$ is less compared to that of $(0/90)_n$ and $d_s/b_s = 2$, while it is more for other values of d_s/b_s ratios. With the increase in stiffener depth the buckling load increases up to certain value and decreases thereafter in case of cross-ply arrangement while it increases and does not drop down in case of angle-ply arrangement.

Table 9 Non-dimensional buckling load of cross-ply laminated shell panel with cross-ply laminated stiffener

Lamination (Shell panel/Stiffener)	(d_s/b_s) ratio	Flat plate	Cylindrical panel	Spherical panel	Hyperbolic hyperboloid panel
$(0/90)_1$	2	30.242	87.249	139.001	28.357
	4	51.961	87.354	139.015	50.603
	6	51.999	87.234	138.648	50.641
	8	51.829	86.768	112.516	50.491
$(0/90)_2$	2	46.547	154.154	226.849	44.047
	4	104.371	154.138	226.698	97.899
	6	119.865	153.712	212.964	116.826
	8	113.870	113.886	112.928	116.144
$(0/90)_3$	2	49.226	166.470	242.790	46.669
	4	105.400	166.430	242.610	98.808
	6	132.316	165.951	213.123	129.052
	8	113.948	113.964	112.996	116.250
$(0/90)_4$	2	50.073	170.717	248.360	47.505
	4	105.179	170.751	248.170	98.606
	6	136.680	170.250	213.185	133.357
	8	113.980	113.996	113.023	116.283

Table 10 Non-dimensional buckling load of angle-ply laminated shell panel with angle-ply laminated stiffener

Lamination (Shell panel/Stiffener)	(d_s/b_s) ratio	Flat plate	Cylindrical panel	Spherical panel	Hyperbolic hyperboloid panel
$(45/-45)_1$	2	33.406	111.530	132.026	34.481
	4	39.887	126.283	175.215	39.385
	6	52.897	126.077	183.267	49.838
	8	72.565	125.328	182.087	65.668
$(45/-45)_2$	2	59.383	196.003	212.475	56.766
	4	63.645	243.136	265.487	60.434
	6	75.501	296.434	327.062	70.494
	8	95.790	324.427	335.345	87.251
$(45/-45)_3$	2	61.072	206.283	222.577	60.062
	4	65.414	254.039	275.656	63.568
	6	77.831	310.666	347.772	73.514
	8	99.466	348.480	360.197	90.273
$(45/-45)_4$	2	63.190	209.863	226.097	61.183
	4	67.453	257.775	279.178	64.637
	6	79.813	315.470	354.877	74.543
	8	101.443	354.823	368.940	91.298

3.2.4 Dynamic instability

After obtaining the free vibration and static buckling characteristics it is now pertinent to study the dynamic instability of stiffened shell panels. In all the dynamic stability analysis, the non-dimensional buckling load of the four layered cross-ply $(0/90)_2$ stiffened flat plate with $(0/90)_2$ stiffener ($d_s/b_s = 4$) is taken as the reference load, so as to plot the instability zones. The effect of parameters like lamination scheme, eccentricity of stiffener and the stacking sequence are presented taking the case of spherical shell panel with a single stiffener $(xst)_b$ attached to the bottom edge. The stiffener depth to breadth ratio (d_s/b_s) is kept as 4 and the static load factor (α) is 0.2 in all cases. The dynamic load factor β varies from 0.0 to 1.5.

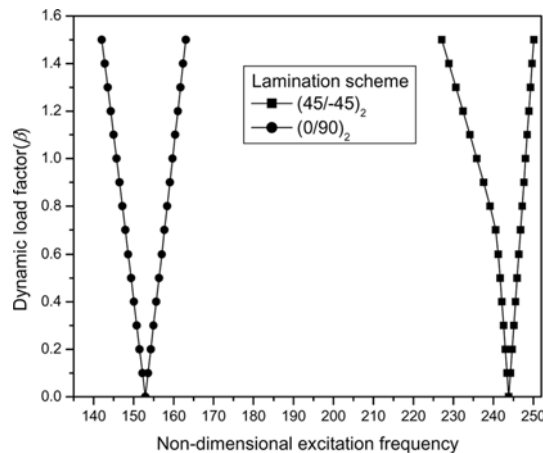


Fig. 12 Effect of lamination scheme on dynamic instability region on spherical shell

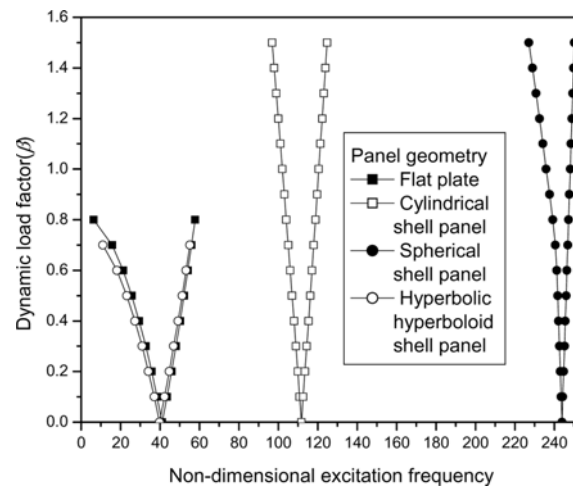


Fig. 13 Effect of geometry on dynamic instability regions

3.2.4.1 Effect of lamination scheme

The effect of lamination scheme on the excitation frequencies of stiffened spherical shell panel is presented in this section. The lamination schemes are $(0/90)_2$ and $(45/-45)_2$. The plots of the dynamic instability region (DIR) are shown in the Fig. 12.

It is observed that for $(45/-45)_2$ lamination scheme the instability region shifts to the higher frequency zone in comparison to $(0/90)_2$ lay up. The plot shows that the onset of instability appears early for cross-ply scheme for stiffened spherical shell panel, indicating that the angle-ply lay up is more dynamically stable than the cross-ply scheme for the given stiffener configuration of the shell panel.

3.2.4.2 Effect of geometry of the shells

The comparison of the dynamic instability regions for $(45/-45)_2$ stiffened plate, cylindrical shell, spherical shell and hyperbolic hyperboloid shell are presented in this section. The plots are shown in the Fig. 13.

It is observed that the DIR for the spherical shell is at the highest frequency zone and the width of the instability region is smaller in this case as compared to the other cases. The DIR gradually shifts to the lower frequency zone side for cylindrical shell, hyperbolic hyperboloid shell and plate respectively. This behaviour indicates that for a given ply lay up and stiffener configuration, the spherical stiffened shell panel is dynamically more stable in comparison to the other panel geometries.

3.2.4.3 Effect of eccentricity of the stiffener

The eccentricity of the stiffener has its effect on the dynamic instability region of the stiffened shell. To illustrate this a $(45/-45)_2$ stiffened spherical shell panel with stiffener with bottom and top eccentricity is analyzed. From the plot (Fig. 14), it is observed that the width of the instability region is higher for the eccentric top stiffener.

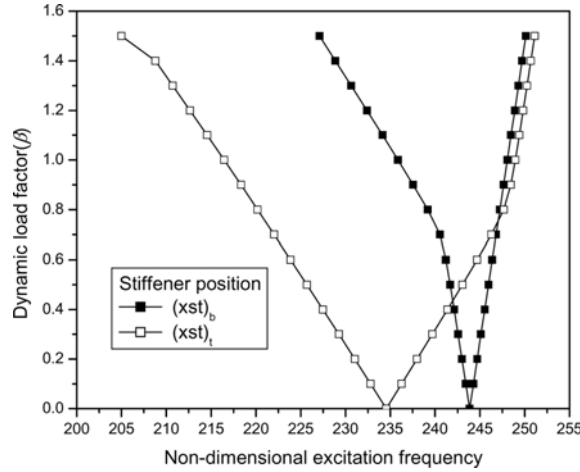


Fig. 14 Effect of eccentricity of the stiffener on dynamic instability region of spherical shell

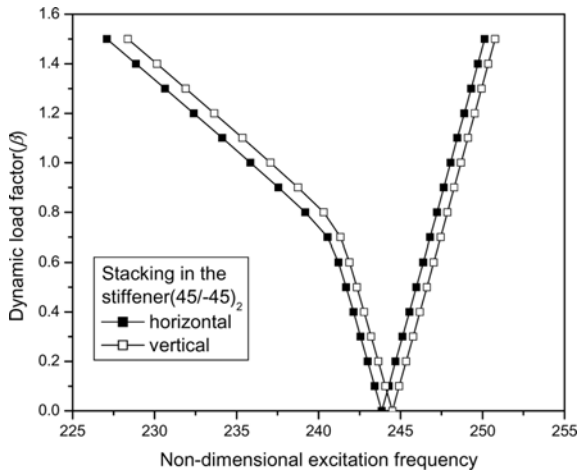


Fig. 15(a) Effect of stacking in stiffener on dynamic instability region of the spherical shell panel for $(45/-45)_2$ lamination scheme in the stiffener

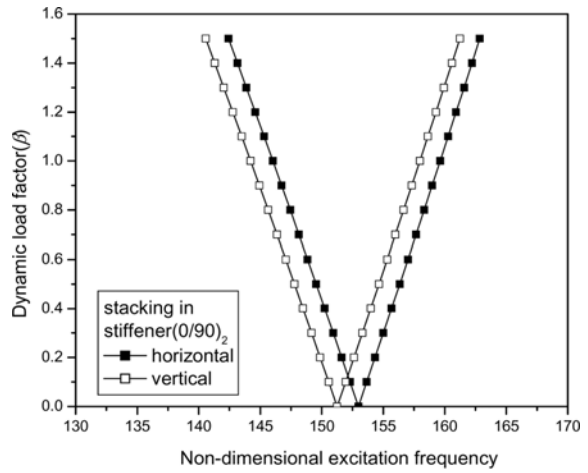


Fig. 15(b) Same as Fig. 15(a) but for $(0/90)_2$ lamination scheme in the stiffener

3.2.4.4 Effect of stacking in stiffener

The effect of the stacking of layers in the stiffener on dynamic instability region of the spherical stiffened shell panel is presented in this section (Fig. 15). The stiffener is eccentric to bottom surface.

In the vertical stacking the dynamic instability region shifts a little to the higher frequency zone side and the width of the instability regions are similar in the case of $(45/-45)$ lamination scheme. But in the case of $(0/90)$ lamination scheme the dynamic instability region shifts a little to the higher frequency zone side for horizontal stacking in the stiffener and here also the instability regions are almost same. This indicates that the stacking scheme of the stiffener has very little effect

on the dynamic instability behaviour for the particular geometry and stiffener scheme of the spherical shell panel.

3.2.4.5 Effect of stiffener scheme

To find out the effect of number of stiffeners on dynamic instability region a spherical shell with $(45/-45)_2$ panel skin and stiffeners are taken. Four sets of stiffener are placed in both the directions. Set one is of one stiffener in both direction at position of y-stiffener at $x = 0$ and x-stiffener at $y = 0.5b$. Set two (Fig. 16) is of three stiffeners in both direction at position of y-stiffener at $x = -0.125a, 0$ and $0.125a$ and x-stiffener at $y = 0.375b, 0.5b$ and $0.625b$. Set three is of five stiffeners in both direction at position of y-stiffener at $x = -0.25a, -0.125a, 0, 0.125a$ and $0.25a$ and x-stiffener at $y = 0.25b, 0.375b, 0.5b, 0.625b$ and $0.75b$. Set four is of seven stiffeners in both direction at position of y-stiffener at $x = -0.375a, -0.25a, -0.125a, 0, 0.125a, 0.25a$ and $0.375a$ and x-stiffener at $y = 0.125b, 0.25b, 0.375b, 0.5b, 0.625b, 0.75b$ and $0.875b$. The dynamic instability regions are plotted in the Fig. 17.

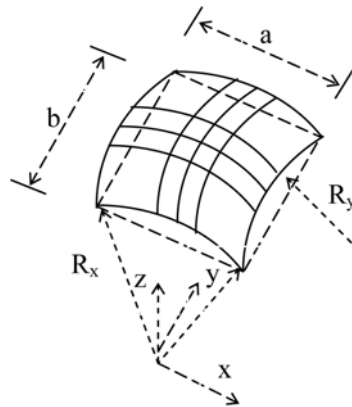


Fig. 16 Stiffened spherical shell panel with three $(xst)_b$ and three $(yst)_b$ stiffeners

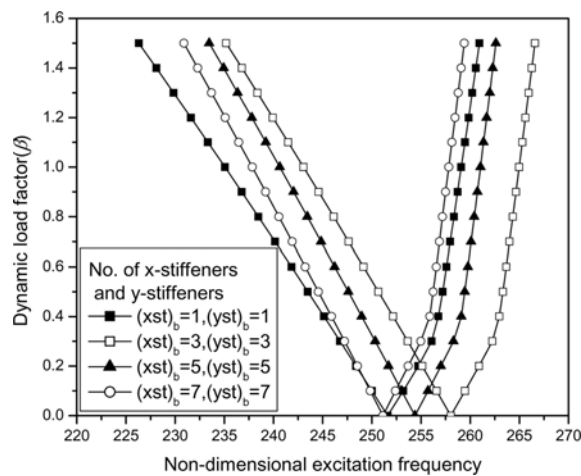


Fig. 17 Effect of stiffener scheme on dynamic instability region of the spherical shell panel

It is observed from Fig. 17 that the dynamic instability zone for the stiffener arrangement of set two ($(xst)_b = 3$ and $(yst)_b = 3$) is at the higher frequency zone side. It indicates that this arrangement is dynamically more stable in comparison to the other stiffener schemes.

4. Conclusions

Based on the observations in the present study the following conclusions can be made.

1. The proposed finite element model consists of an eight-noded isoparametric degenerated shell element and a compatible three-noded curved beam element for the representation of shell skin and stiffeners respectively. It has exhibited very good performance in terms of accuracy and convergence without involving any numerical disturbance.
2. In most of the cases the non-dimensional buckling loads and frequencies are higher for angle-ply (45/-45/45/-45/---) stiffened shell panels in comparison to the cross-ply (0/90/0/90/---) lamination scheme.
3. The stiffened panel with angle-ply lay up is dynamically more stable than the cross-ply scheme for the given geometry and stiffener configuration of the shell panel.
4. For a given ply lay up and stiffener configuration, the spherical stiffened shell panel is dynamically more stable in comparison to the other panel geometries.
5. With regard to dynamic instability, for the given stiffener and lamination scheme it is better to place the stiffener in the bottom surface of the spherical shell panel.
6. In case of vertical stacking scheme the onset of dynamic instability region shifts a little to the higher frequency zone side for (45/-45)₂ lamination scheme and a little lower frequency zone side for (0/90)₂ lamination scheme for the spherical stiffened shell.
7. For the stiffened spherical shell panel with three stiffeners in each direction, the dynamic instability zone is at higher frequency zone in comparison to other stiffener arrangement.

References

- Ahmad, S. (1970), "Analysis of thick and thin shell structures by curved finite elements", *Int. J. Num. Met. Eng.*, **2**, 419-451.
- Aksu, G. (1982), "Free vibration of stiffened plates including the effect of in plane inertia", *J. Appl. Mech., Trans of ASME*, **49**, 206-212.
- Bathe, K.J. (1996), *Finite Element Procedure*, Prentice-Hall of India Private Limited, New Delhi.
- Bhimaraddi, A., Carr, A.J. and Moss, P.J. (1989), "Finite element analysis of laminated shells of revolution with laminated stiffeners", *Comput. Struct.*, **33**(1), 295-305.
- Bolotin, V.V. (1964), *The Dynamic Stability of Elastic Systems*, Holden-day, Inc.
- Chao, C.C. and Lee J.C. (1980), "Vibration of eccentrically stiffened laminates", *J. Composite Materials*, **14**, 233-244.
- Chattopadhyay, B., Sinha, P.K. and Mukhopadhyay, M. (1992), "Finite element free vibration analysis of eccentrically stiffened composite plates", *J. of Reinforced Plastics and Composites*, **11**(10), 1003-1034.
- Chen, L.W. and Yang, J.Y. (1990), "Dynamic stability of laminated composite plates by finite method", *Comput. Struct.*, **36**(5), 845-851.
- Duffield, R.C. and Willems, N. (1972), "Parametric resonance of stiffened rectangular plates", *J. Appl. Mech.*, **39**, 217-226.
- Ferguson, G.H. and Clark, R.D. (1979), "A variable thickness curved beam and shell stiffener with sheat

- deformation", *Int. J. Num. Met. Eng.*, **14**, 581-592.
- Harik, I.E. and Guo, M. (1993), "Finite element analysis of eccentrically stiffened plates in free vibration", *Comput. Struct.*, **49**(6), 1007-1015.
- Hutt, J.M. and Salam, A.E. (1971), "Dynamic stability of plates by finite element method", *J. Eng. Mech.*, ASCE, **97**, 897-899.
- Kidane, S., Lia, G., Helmsa, J., Panga, S. and Woldesenbet, E. (2003), "Buckling load analysis of grid stiffened composite cylinders", *Composite Part B: Engineering*, **34**(1), 1-9.
- Kwon, Y.W. (1991), "Finite element analysis of layered composite plates using a higher order bending theory", *Comput. Struct.*, **38**(1), 57-62.
- Liao, C.L. and Reddy, J.N. (1990), "Analysis of anisotropic, stiffened composite laminates using a continuum-based shell element", *Comput. Struct.*, **34**(6), 805-815.
- Liao, C.L. and Cheng, C.R. (1994), "Dynamic stability of stiffened laminated composite plates and shells subjected to in plane pulsating forces", *J. Sound Vib.*, **174**(3), 335-351.
- Mermertas, M. and Belek, H.T. (1991), "Dynamic stability of radially stiffened annular plates", *Comput. Struct.*, **40**(3), 651-657.
- Merrit, R.G. and Willems, N. (1973), "Parametric resonance of skew stiffened plates", *J. Appl. Mech.*, **40**, 439-444.
- Moorthy, J., Reddy, J.N. and Pault, R.H. (1990), "Parametric instability of laminated composite plates with transverse shear deformation", *Int. J. Solids Struct.*, **26**(7), 801-811.
- Mukherjee, A. and Mukhopadhyay, M. (1987), "Finite element free vibration of eccentrically stiffened plates", *Comput. Struct.*, **30**(6), 1303-1317.
- Mukhopadhyay, M. (1989), "Vibration and stability analysis of stiffened plates by semi-analytic finite difference method, Part-I: Consideration of bending displacement only", *J. Sound Vib.*, **130**(1), 27-39.
- Nayak, A.N. and Bandyopadhyay, J.N. (2002), "On free vibration of stiffened shallow shells", *J. Sound Vib.*, **255**(2), 357-382.
- Olson, M.D. and Hazell, C.R. (1977), "Vibration studies of some integral rib-stiffened plates", *J. Sound Vib.*, **50**, 43-61.
- Panda, S.C. and Natarajan, R. (1979), "Finite element analysis of laminated composite plates", *Int. J. Num. Met. Eng.*, **14**, 69-79.
- Prusty, B.G. (2001), "Static, dynamic, buckling and failure analysis of composite stiffened shell structures, a finite element approach", PhD thesis, Indian Institute of Technology, Kharagpur.
- Rao, J.S. (1999), *Dynamics of Plates*, Narosa Publishing House, New Delhi.
- Reddy, J.N. and Starnes, J.H. Jr (1993), "General buckling of stiffened circular cylindrical shells according to a layerwise theory", *Comput. Struct.*, **49**(4), 605-616.
- Rikards, R., Chate, A. and Ozolinsh, O. (2001), "Analysis for buckling and vibrations of composite stiffened shells and plates", *Compos. Struct.*, **51**(4), 361-370.
- Samanta, A. and Mukhopadhyay, M. (2004), "Free vibration of stiffened shells by the finite element technique", *European J. of Mechanics A/Solids*, **23**, 159-179.
- Sciuva, M.D. and Crrera, E. (1990), "Static buckling of moderately thick, anisotropic, laminated and sandwich cylindrical shell panels", *AIAA J.*, **28**, 1782-1793.
- Sivasubramonian, B., Rao, G.V. and Krishnan, A. (1999), "Free vibration longitudinally stiffened curved panels with cutouts", *J. Sound Vib.*, **226**, 41-55.
- Srinivasan, R.S. and Chellapandi, P. (1986), "Dynamic stability of rectangular laminated composite plates", *Comput. Struct.*, **24**(2), 233-238.
- Srivastava, A.K.L., Datta P.K. and Sheikh, A.H. (2002), "Vibration and dynamic stability of stiffened plates subjected to in-plane harmonic edge loading", *Int. J. Str. Stability and Dynamics*, **2**(2), 185-206.
- Thomas, J. and Abbas, B.H.A. (1983), "Vibration characteristics and dynamic stability of stiffened plates", *AIAA J.*, **21**, 277-285.
- Timoshenko, S.P. and Gere, J.M. (1961), *Theory of Elastic Stability*, Tokyo, McGraw-hill, Kogakusha.
- Timoshenko, S.P. and Goodier, J.M. (1951), *Theory of Elasticity*, Tokyo, McGraw-hill, Kogakusha.
- Wu, D.L. and Zhang, Z. (1991), "Nonlinear buckling analysis of discretely stiffened cylindrical shells", *Compos. Struct.*, **18**(1), 31-45.

- Zeng, H. and Bert, C.W. (2001), "A differential quadrature analysis of vibration for rectangular stiffened plates", *J. Sound Vib.*, **241**(2), 247-252.
- Zienkiewicz, O.C. (1977), *The Finite Element Method*, Tata Mc-Graw Hill Publishing Company Limited, New Delhi.

Notation

$\xi-\eta-\zeta$: curvilinear coordinate system
$x-y-z$: global cartesian coordinate system
$x'-y'-z'$: local coordinate system
a, b	: base dimensions of the stiffened panels
b_s, d_s	: breadth (web thickness) and depth of stiffener
DIR	: dynamic instability region
$(xst)_b$: stiffener in x -direction in bottom surface
$(xst)_t$: stiffener in x -direction in top surface
$(yst)_b$: stiffener in y -direction in bottom surface
$(yst)_t$: stiffener in y -direction in top surface
$[K]$: combined elastic stiffness matrix of panel and stiffeners
$[M]$: combined mass matrix of panel and stiffeners
$[K_G]$: combined geometric stiffness matrix of panel and stiffeners
N_i	: quadratic serendipity shape functions shell element
N_{si}	: quadratic shape functions stiffener element
Ω	: excitation frequency of the load
α	: static load factor
β	: dynamic load factor
β_s	: shear correction factor
β_t	: torsion correction factor